Chinese Science Bulletin 2005 Vol. 50 No. 13 1395—1403

SHRIMP zircon U-Pb geochronology of Indosinian granites in Hunan Province and its petrogenetic implications

WANG Yuejun[1], FAN Weiming[1], LIANG Xinquan[1], PENG Touping[1] & SHI Yuruo[2]

1. Key Laboratory of Isotope Geochronology and Geochemistry, Guangzhou Institute of Geochemistry, Chinese Academy of Sciences, Guangzhou 510640, China;
2. SHRIMP Isotope Laboratory, Chinese Academy of Geological Sciences, Beijing 100037, China

Correspondence should be addressed to Wang Yuejun (email: yjwang@gig.ac.cn)

Abstract The SHRIMP zircon U-Pb geochronology of three typically Indosinian granitic plutons with peraluminous and potassium-rich affinities (Tangshi ultraunit for Weishan and Baimashan, and Longtan ultraunit for Guandimiao) is presented in Hunan Province, South China. The analyses of zircons from biotite monozonite granites for Weishan, Baimashan and Guandimiao plutons show the single and tight clusters on the concordia, and yield the weighted mean $^{206}Pb/^{238}U$ ages of 244±4, 243±3 and 239±3 Ma, respectively, representing the crystallized ages of these Indosinian granites. These data suggest that the Indosinian granitic plutons as previously thought formed at a narrow age span. In combination with other data, it is inferred that the Indosinian granites within the South China Block probably distributed in Hunan, Jiangxi, Guangxi and Guangdong provinces as planar shape, and were the derivation of the crustal materials in the intracontinental thickening setting. These precisely geochronological data provide important constraints for better understanding the spatiotemporal pattern of the Indosinian peraluminous granites and early Mesozoic tectonic evolution of the South China Block.

Keywords: SHRIMP zircon U-Pb geochronology, Indosinian granites, Hunan.

DOI: 10.1360/982004-603

The structure, magmatism and sedimentation within the South China Block (SCB) related to the Indosinian Orogeny had attracted considerable attention since Deprat[1] and Fromagat[2] proposed the "Indosinian movement" based on two unconformities between Pre-Norian and Pre-Rhaetian during Triassic in Vietnam. However, Indosinian tectonic evolution of the SCB has been long debated[3−6]. Some researchers believed that the complicated structure-magmatism-sedimentation within the SCB was related to the subduction of an oceanic plate and subsequent collision within the SCB during Indosinian episode[3,4]. Other researchers considered that these geological phenomena were the result of the westward subduction of the Pacific plate during early Mesozoic[5,6]. Guo[7] even suspected the occurrence of the Indosinian Orogeny within the SCB. To advance our understanding of the Indosinian Orogeny and early Mesozoic tectonic evolution of the SCB, it is important to precisely date the representative granitoids related to the Indosinian orogeny within the SCB and to probe their petrogenesis.

A series of studies have been undertaken for the Indosinian granitoids within the SCB since 1970s. These studies revealed that the Indosinian granitoids within the SCB mainly exposed in Hunan and Guangxi provinces. They are composed of strongly peraluminous to metaluminous potassic-rich granitoids, monzonitic granitoids and granodiorites, and their formation was closely related to the collision between the Yangtze and Cathaysian blocks in petrogenesis as previously thought[3,6,8]. However, these granitoids mainly distributed in the central part of the SCB, far from the collisional boundary. The spatial distribution is distinct from that of magmatism occurring in convergent margin. The Indosinian granitoids in Hunan Province, representatives of the contemporaneous granitoids within the SCB, are generally in large volume and occur as laccoliths and batholiths along deep-fault planes or fault intersections[9] (Fig. 1). They are strongly to slightly peraluminous with A/CNK>1.00, and show LREE-enriched chondrite-normalized REE patterns with strongly negative Eu anomalies (δEu=0.18−0.56). ($^{87}Sr/^{86}Sr$) ratios are in a range of 0.7136−0.7239, $\varepsilon_{Nd}(t)$ of −9—−14 and δO^{18} of 8.35‰−17.36‰[9−12]. These features are distinct from those of early Mesozoic granodiorites (170−180 Ma) interpreted as melting product of the underplating basaltic rocks hybridized with the old crustal materials. Thus these Indosinian granites in Hunan Province have important implications for Indosinian tectonic evolution in the SCB.

The previously geochronological data from mineral K-Ar, monazite U-Th-Pb, whole-rock Rb-Sr and zircon U-Pb methods for the Indosinian granites in Hunan Province gave the age range of 163−267 Ma[9], unsuitably exploring the spatiotemporal distribution of the Indosinian granites within the SCB. Xu et al.[13] obtained the single zircon LA-ICPMS U-Pb ages of 236−239 Ma from Luxi and Xiazhuang plutons from Guidong complex. Deng et al.[14] reported the SHRIMP zircon U-Pb ages of 233, 230 and 236 Ma for Darongshan, Jiuzhou and Taima plutons in southeastern Guangxi. These high-precision zircon U-Pb geochronological data indicate that these granites within the SCB traditionally classified as peraluminous Hercynian-Indosinian granites most likely formed during early Indosinian with a narrow age span and exposed at not only Hunan and Guangxi but also Jiangxi, Guangdong and Hainan provinces[13,14],1). With aims to better characterize the spatiotemporal distribution of the Indosinian granites and their petrogenesis, and further understand early Mesozoic tectonic evolution of the SCB, this paper presents a set of SHRIMP zircon U-Pb geochronological data for three typically Indosinian granitic plutons (Weishan, Guandimiao and Baimashan) in Hunan Province.

1 Geological background and petrography

There existed voluminous Indosinian intermediate-acid (mainly granitic) plutons in Hunan Province. These plutons (~5600 km^2 exposed acreage), as a planar-shape, outcropped at the region bounded between the Chenzhou-Linwu and Xupu-Jinxian faults (Fig. 1). The typical plutons include Cangshuipu, Weishan, Dashenshan, Baimashan, Ziyunshan, Xiema, Guandimiao, Wawutang, Tashan, Yangmingshan, Dayishan, Jilongjie, Jiangjunmiao, Chuankou and Wufengxian plutons. They occurred as stocks and batholiths, and intruded Neoproterozoic-Devonian strata, even upper Permian sequence (Fig. 1), e.g. the Indosinian granites were overlain by upper Permian marble at the eastern Wufengxian pluton[9–11].

Previously geochronological data for these Indosinian granites from mineral K-Ar, monazite U-Th-Pb, whole-rock Rb-Sr and zircon U-Pb methods gave a wide range of 163—267 Ma[9] with a peak age of 185—232 Ma[9–12]. Lithologically, these Indosinian granites are mainly composed of peraluminous and potassium-rich hornblende-biotite monzonitic granite, biotite monzonitic granite, two-mica granites, hornblende-biotite granite and garnet-muscovite granites. The biotite granodiorite in several plutons is observed. These rocks show porphyritic or granitic textures of mediated- to fined-grained sizes (1—5 mm). The phenocryst is commonly constituted by subeuhedral to euhedral feldspar (1—2.5 cm), and the matrix is

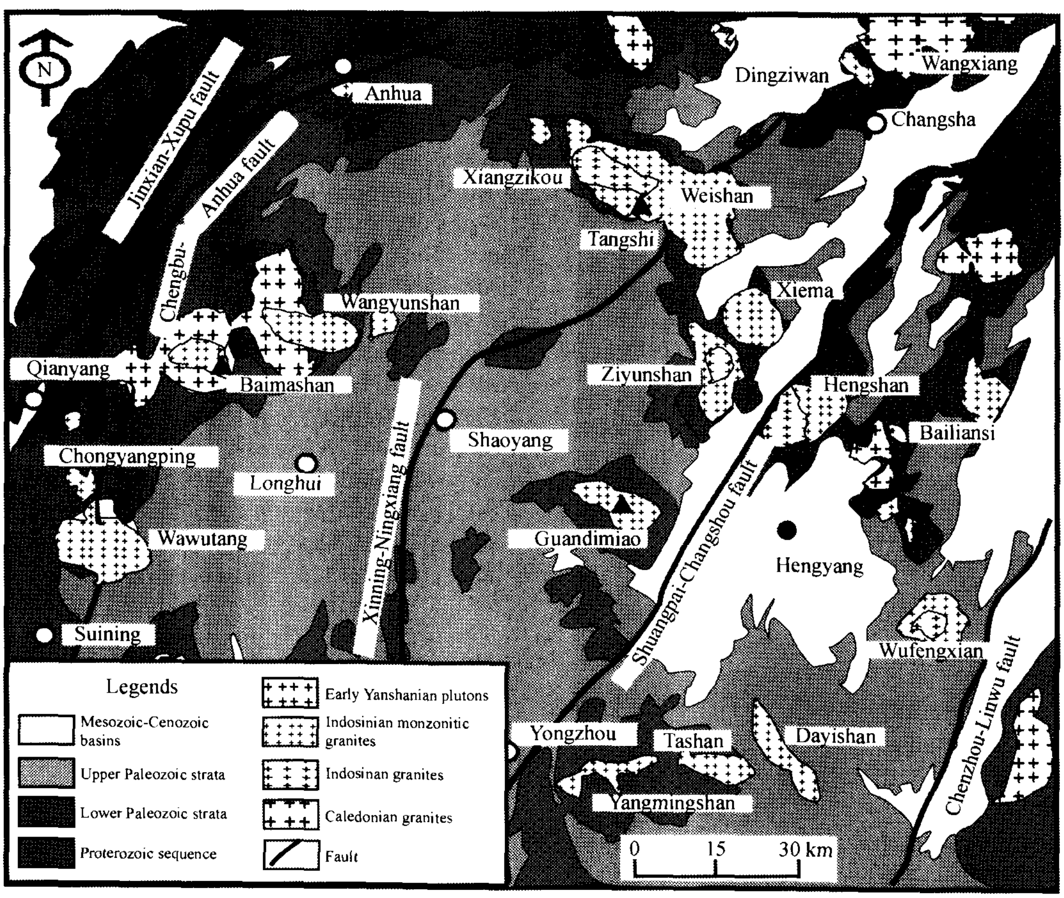

Fig. 1. Geological map showing the distribution of the Indosinian granites in Hunan Province[9]. Triangle symbols note the sampling locations of SHRIMP zircon U-Pb dating.

1) Ge, X. Y., Mesozoic magmatism in Hainan island (SE China) and its tectonic implications: Geochronology, Geochemical and Sr-Nd Isotope Evidences (in Chinese), PhD thesis, Guangzhou Institute of Geochemistry, Chinese Academy of Sciences, 2003, 1—83.

mainly composed of xenomorphic fine-grained (1—4 mm) feldspar, plagioclase with normal oscillatory zoning, quartz and a few subeuhedral to euhedral biotite and opaque oxides. In several plutons, there are additional phenocryst and matrix. For example, the phenocrysts included additional plagioclase in Weishan and Guandimiao plutons, and additional amphibole for matrix in Jilongjie and Wufengxian plutons. The compressional deformation signatures, e.g. undulatory extinction of quartz, kinking and fracture of plagioclase and bending of biotite, are observed in these plutions.

Three typically Indosinian granitic plutons of Weishan, Guandimiao and Baimashan in the central part of Hunan Province are selected for SHRIMP zircon U-Pb dating in this study (Fig. 1). Weishan pluton (~1240 km^2) is situated at the border of Ningxiang, Shaoshan, Xiangxiang and Anhua counties, and is composed of Tangshi ultraunit dominated by biotite±hornblende monzonitic granite and Xiangzikou ultraunit by two-mica monzonitic granite[15]. The mineral lineation and lamellation comprised of preferentially oriented feldspar phenocrysts are commonly observed in Tangshi ultraunit[10−12,15]. Guandimiao pluton (~290 km^2) located at the border of Hengyang, Qidong and Shaodong counties is composed of E-W-trending Tangshi ultraunit (biotite monzonitic granite) and WNW-trending Xiangzikou ultraunit (two-mica monzonitic granite)[15]. Baimashan pluton of over 1600 km^2 is located at the border of Xinhua, Longhui and Xupu counties, and is a complex composed of Silurian Shuiche, middle Triassic Longtan, upper Triassic Xiaoshajiang and lower Jurassic Longzangwan ultraunits[12,15]. In Shuiche and Longtan ultraunits, there usually occurred quartz dioritic xenoliths experiencing strongly compressional deformation. The granites in Xiaoshajiang ultraunit commonly developed gneissic texture, which was distinct from those in Longzangwan ultraunit with insignificant structural overprinting[10−12,15].

2 Analytical methods

Zircons were separated from the fresh samples by using conventional heavy liquid and magnetic techniques and purified by handpicking under a binocular microscope. Only those idiomorphic zircon grains free of inclusions and cracks were selected for SHRIMP U-Pb dating. These zircons were mounted in epoxy, polished, and coated with gold. The mounts were then photographed in transmitted and reflected light for identification of analyzed grains. The internal structure of zircons was examined with the cathodoluminescence (CL) image technique prior to U-Pb isotopic analyses. The U-Pb isotopic determination was undertaken on the polished mount with a sensitive high-resolution ion microprobe (SHRIMP II) at the Institute of Geology, Chinese Academy of Geological Sciences. Detailed analytical procedures of SHRIMP are similar to those described in refs. [16,17]. The standard TEM zircons (age of 417 Ma) of RSES were used to determine the elemental discrimination that occurs during sputter ionization. The calculation of $^{206}Pb/^{238}U$ ages is based on the assumption that the bias in the measured $^{206}Pb/^{238}U^+$ ratio can be described by the same power law relationship between $^{206}Pb/^{238}U^+$ and UO^+/U^+ for both the zircon standard and sample. Common Pb correction was made by using the observed ^{204}Pb peak[18]. Data processing was carried out with the SQUID 1.03 and Isoplot/Ex 2.49 programs of Ludwig (2001)[19].

3 Sample description and results

The samples 02QSH06, 01GD09 and 02JSH03 for SHRIMP zircon U-Pb dating are representatives of Tangshi untraunit for Weishan and Guandimiao plutons and Longtan ultraunit for Baimashan pluton, respectively. Sample 02QSH06, lithologically porphyritic biotite monzonitic granite with the feldspar phenocryst, is collected from Qingshanqiao, Ningxiang County. The mineral compositions are ~25% feldspar, ~32% plagioclase, ~38% quartz, ~5% biotite and minor amount of euhedral sphene, apatite, zircon, Fe-Ti oxides and allanite. Sample 01GD09 is porphyritic biotite monzonitic granite, and is taken from Guandimiao, Qidong County. Its mineral constitutes are ~33% feldspar, ~30% plagioclase, ~30% quartz, ~7% biotite and minor amount of euhedral sphene, apatite, zircon, Fe-Ti oxides and allanite. Sample 02JH03 is a medium- to fined-grained biotite monzonitic granite from Jinchangping Village, which is mainly composed of ~45% plagioclase, ~16% feldspar, ~37% quartz, and ~8% biotite. These granites are slightly to strongly peraluminous (A/CNK = 1.05—1.13) and are characterized by high K_2O content with $K_2O>Na_2O$. The granites in Longtan ultraunit for Baimashan pluton exhibit higher MgO and CaO and lower K_2O and SiO_2 than those in Tangshi ultraunit for Weishan and Guandimiao plutons as illustrated in Table 1. The results of SHRIMP zircon U-Pb dating for three samples from Weishan, Guandimiao and Baimashan plutons are listed in Table 2, and cathodoluminescence (CL) images for representative zircons are shown in Fig. 2 (see Fig. 1 for locations of samples).

Zircons from these samples exhibit similar morphology, being mostly euhedral and up to 150—350 μm in length with ~2∶1—4∶1 of length/width ratio. Most crystals are light brown and brown, prismatic and transparent to subtransparent. Zircons from samples 02QS06 and 02JH03 exhibit well-developed {100} and {111} crystal faces, and some zircons from sample 01GD09 have additionally well-developed {110} and {311} crystal faces. The internal structure revealed by the CL images shows that some zircons have the core with heterogeneously spotted and estuary texture and the edge with weak oscillatory zoning, similar to those of recrystallized magmatic zircon. Most zircons exhibit the internal structure with small core and edge of strong oscillatory zoning, similar to that of typical

Table 1 Major oxides composition for representative Indosinian granites (wt%)

	Tangshi ultraunit, Weishan				Tangshi ultraunit, Guandimiao			Longtan ultraunit, Baimashan		
	02QSH02	02QSH06	02TSH01	02TSH05	01GD01	01GD09	01GD18	02JSH03	02JSH05	02JSH07
SiO_2	70.64	70.61	73.34	73.71	71.59	71.81	71.51	69.96	68.81	69.95
Al_2O_3	14.5	14.03	13.88	13.70	14.04	13.90	14.55	14.36	13.87	14.77
Fe_2O_3	0.42	0.44	0.11	0.14	0.26	0.21	0.49	0.28	0.38	0.30
FeO	2.32	2.37	1.55	1.60	2.13	2.03	1.76	2.33	2.57	2.33
MgO	1.18	1.21	0.70	0.72	1.33	1.25	1.24	1.56	2.30	1.60
CaO	2.71	2.06	1.82	1.45	2.27	2.14	2.23	2.92	3.23	2.96
Na_2O	3.16	2.59	2.77	2.94	2.71	2.71	2.87	2.82	2.23	2.78
K_2O	3.25	4.72	4.38	4.38	4.04	4.36	3.81	3.14	3.44	3.77
MnO	0.05	0.06	0.03	0.04	0.04	0.05	0.05	0.05	0.14	0.05
TiO_2	0.38	0.40	0.24	0.24	0.34	0.33	0.34	0.39	0.83	0.40
P_2O_5	0.11	0.12	0.09	0.08	0.14	0.12	0.10	0.12	0.21	0.11
LOI	0.99	1.19	0.84	0.75	0.79	0.62	0.60	0.67	0.99	0.52
Total	99.71	99.8	99.75	99.75	99.68	99.53	99.55	98.6	99.8	99.54
A/CNK	1.06	1.07	1.10	1.12	1.08	1.06	1.13	1.07	1.14	1.05
K_2O/Na_2O	1.03	1.82	1.58	1.49	1.49	1.61	1.33	1.11	1.45	1.36

A/CNK=Al_2O_3/($CaO+Na_2O+K_2O$) (molecular).

Table 2 SHRIMP U-Pb analyses of zircons for three Indosinian granites in Hunan Province

Spot	U (ppm)	Th (ppm)	$^{232}Th/^{238}U$	ppm $^{206}Pb^*$	$^{238}U/^{206}Pb^*$	$^{207}Pb^*/^{206}Pb^*$ ±%	$^{207}Pb^*/^{235}U$ ±%	$^{206}Pb^*/^{238}U$ ±%	discordant (%)	$^{206}Pb/^{238}U$ ±1σ Ma	$^{207}Pb/^{235}Pb$ ±1σ Ma	$^{207}Pb/^{206}Pb$ ±1σ Ma
Biotite monozonite granite, Weishan (Tangshi ultraunit): 02QSH06												
HC1.1	1589	389	0.25	50.5	27.09	0.0488±2.4	0.2481±3.7	0.0369±2.8	−72	233.7±6.4	225.0±7.5	136±56
HC2.1	3811	799	0.22	131	25.08	0.0495±1.5	0.2720±3.1	0.0399±2.7	−48	252.1±6.8	244.3±6.7	170±36
HC3.1	3133	598	0.20	104	25.88	0.0503±2.0	0.2680±3.4	0.0386±2.7	−17	244.4±6.6	241.1±7.3	210±46
HC4.1	4918	839	0.18	176	24.11	0.0503±1.2	0.2877±3.0	0.0415±2.7	−25	262.0±7.0	256.7±6.8	209±29
HC5.1	3148	546	0.18	107	25.38	0.0493±1.6	0.2676±3.2	0.0394±2.8	−56	249.1±6.7	240.8±6.9	160±38
HC6.1	4866	552	0.12	170	24.81	0.0490±2.6	0.2720±3.8	0.0403±2.8	−72	254.7±6.9	244.3±8.3	148±61
HC7.1	1758	406	0.24	58.0	26.23	0.0499±2.5	0.2621±3.7	0.0381±2.8	−28	241.2±6.5	236.4±7.8	189±57
HC8.1	5212	765	0.15	191	23.47	0.0506±1.4	0.2972±3.0	0.0426±2.7	−21	269.0±7.2	262.2±7.0	222±30
HC9.1	4337	852	0.20	168	23.56	0.0584±6.7	0.3020±7.2	0.0424±2.8	51	267.8±7.3	267.4±19	544±150
HC10.1	2866	519	0.19	95.2	26.56	0.0523±4.7	0.2720±5.4	0.0377±2.8	21	238.3±6.5	244.0±12	300±110
HC10.2	2175	417	0.20	69.8	27.06	0.0482±3.8	0.2450±4.7	0.0370±2.8	−118	233.9±6.4	222.5±9.4	107±90
HC11.1	2125	440	0.21	69.5	26.68	0.0499±4.1	0.2580±5.0	0.0375±2.8	−25	237.2±6.4	233.0±10	190±96
HC12.1	3032	444	0.15	105	24.94	0.0489±1.6	0.2704±3.2	0.0401±2.8	−76	253.4±6.8	243.0±6.9	144±37
HC13.1	1556	565	0.38	51.5	26.12	0.0483±3.2	0.2550±4.2	0.0383±2.8	−117	242.2±6.6	230.6±8.7	112±76
HC14.1	1735	626	0.37	59.2	25.30	0.0486±2.4	0.2647±3.7	0.0395±2.8	−98	249.9±6.8	238.4±7.9	126±57
HC15.1	1858	611	0.34	64.8	24.76	0.0503±2.5	0.2800±3.8	0.0404±2.8	−23	255.3±6.9	250.7±7.4	208±59
HC16.1	2896	589	0.21	99.3	25.09	0.0514±1.6	0.2822±3.2	0.0399±2.7	2	252.0±6.8	252.4±7.2	257±36
HC17.1	3952	639	0.17	121	28.46	0.0492±3.3	0.2380±4.3	0.0351±2.8	−43	222.6±6.0	216.8±8.4	155±77
Biotite monozonite granite, Guandimiao (Tangshi ultraunit): 01GD09												
HE1.1	1029	356	0.36	33.4	26.64	0.0486±4.7	0.2510±5.5	0.0375±2.8	−88	237.5±6.6	227.0±11	126±110
HE2.1	1168	605	0.54	38.8	26.12	0.0505±4.3	0.2670+ 5.1	0.0383±2.8	−11	242.2±6.7	240.2±11	218± 99
HE3.1	925	640	0.71	29.1	27.55	0.0506±4.5	0.2531±5.3	0.0363±2.8	−3	229.9±6.4	229.0±11	223±100
HE4.1	6157	13044	2.19	24.8	21.48	0.0516±2.2	0.3310±3.8	0.0466±3.1	−10	293.4±9.0	290.3±9.6	267± 50
HE5.1	1139	610	0.55	38.6	25.61	0.0455±5.1	0.2451±5.8	0.0390±2.8	1003	246.9±6.8	223.0±12	-27±120
HE6.1	475	315	0.69	14.9	27.9	0.0463±11	0.2290±11	0.0359±3.7	−1560	227.1±8.2	209.1±21	14±260
HE7.1	2148	1256	0.60	73.8	25.21	0.0478±3.3	0.2610±4.3	0.0397±2.8	−183	250.8±6.8	235.5±9.0	89± 79
HE8.1	1539	1218	0.82	51.2	26.16	0.0490±4.4	0.2581±5.2	0.0382±2.8	−65	241.8±6.6	233.0±11	146±100

(*To be continued on the next page*)

(*Continued*)

Spot	U (ppm)	Th (ppm)	^{232}Th/^{238}U	ppm ^{206}Pb*	^{238}U/^{206}Pb*	^{207}Pb*/^{206}Pb* ±%	^{207}Pb*/^{235}U ±%	^{206}Pb*/^{238}U ±%	discordant (%)	^{206}Pb/^{238}U ±1σ Ma	^{207}Pb/^{235}Pb ±1σ Ma	^{207}Pb/^{206}Pb ±1σ Ma
HE9.1	721	502	0.72	22.8	27.49	0.0453±8.1	0.2270±8.5	0.0364±2.9	654	230.3±6.5	208.0±16	-42±200
HE101	804	488	0.63	26.6	26.19	0.0477±5.4	0.2510±6.1	0.0382±2.8	−192	241.5±6.7	227.0±12	83±130
HE11.1	1803	808	0.46	61.9	25.09	0.0492±2.4	0.2706±3.7	0.0399±2.8	−58	252.0±6.8	243.1±8.8	159± 56
HE12.1	1348	841	0.64	44.3	26.27	0.0530±2.9	0.2781±4.0	0.0381±2.8	27	240.8±6.6	249.1±8.8	329± 65
HE12.2	1221	598	0.51	40.0	26.44	0.0496±4.2	0.2590±5.0	0.0378±2.8	−35	239.4±6.6	234.0±10	177± 97
HE13.1	1879	845	0.46	63.8	25.46	0.0500±2.8	0.2700±4.0	0.0393±2.8	−29	248.4±6.8	242.7±8.6	193± 66
HE14.2	1418	1082	0.79	47.9	25.63	0.0492±3.9	0.2650±4.8	0.0390±2.8	−59	246.8±6.8	239.0±10	156± 91
Monozonite granite, Baimashan (Longtan ultraunit): 02JSH03												
HA1.1	3292	856	0.27	110	25.64	0.05198±1.4	0.2796±2.7	0.0390±2.4	13	246.7±5.7	250.3±6.0	285±31
HA2.1	1360	407	0.31	48.6	25.18	0.1145±3.8	0.6270±4.5	0.0397±2.4	87	251.1±6.0	494.0±18	1871±68
HA3.1	1691	474	0.29	55.5	26.26	0.0698±4.3	0.3670±5.0	0.0381±2.5	74	241.0±6.0	317.0±14	922±89
HA4.1	2212	460	0.21	74.2	25.68	0.0518±1.8	0.2780±3.0	0.0389±2.4	11	246.3±5.7	249.1±6.6	277±42
HA5.1	3102	821	0.27	106	25.14	0.0527±1.5	0.2890±2.8	0.0398±2.3	20	251.5±5.8	257.8±6.4	315±34
HA6.1	2558	904	0.37	83.0	26.53	0.0518±1.6	0.2691±2.8	0.0377±2.4	14	238.5±5.5	242.0±6.0	276±36
HA7.1	2464	675	0.28	86.6	24.51	0.0513±1.7	0.2884±2.9	0.0408±2.4	−2	253.8±6.0	257.3±6.6	252±39
HA8.1	2032	565	0.29	65.8	26.60	0.0582±1.8	0.3019±3.0	0.0376±2.4	56	237.9±5.5	267.9±7.1	539±39
HA9.1	2100	488	0.24	69.8	25.93	0.0548±2.2	0.2916±3.2	0.0386±2.4	40	244.0±5.7	259.8±7.3	405±49
HA10.1	2132	1157	0.56	72.6	25.42	0.0889±1.8	0.4820±3.0	0.0393±2.4	82	248.8±5.8	399.4±9.9	1402±34
HA11.1	1257	412	0.34	41.2	26.26	0.0541±2.3	0.2840±3.3	0.0381±2.4	36	240.9±5.7	253.9±7.4	375±51
HA11.2	2088	524	0.26	68.9	26.05	0.0523±1.6	0.2768±2.9	0.0384±2.4	19	242.8±5.6	248.1±6.4	299±36
HA12.1	4552	1148	0.26	153	25.58	0.0553±1.1	0.2981±2.6	0.0391±2.3	42	247.2±5.7	264.4±6.1	425±24
HA13.1	1887	772	0.42	64.4	25.30	0.0733±2.1	0.3990±3.2	0.0396±2.4	76	249.9±5.8	340.9±9.3	1022±42
HA14.1	3876	1223	0.33	128	25.98	0.0603±1.3	0.3099±2.7	0.0385±2.3	60	243.5±5.6	258.1±6.7	613±28
HA15.1	1598	550	0.36	57.3	24.15	0.1243±4.1	0.7100±4.8	0.0414±2.4	87	261.5±6.1	545.0±20	2019±73
HA16.1	2815	1721	0.63	95.3	25.42	0.0557±1.6	0.3023±2.8	0.0393±2.4	44	248.7±5.7	261.2±6.6	442±35
HA17.1	2612	620	0.25	92.4	24.44	0.0939±2.0	0.5300±3.1	0.0409±2.4	83	250.5±6.0	432.0±11	1506±38

magmatic zircons (Figs. 2(a)−(c)). Eighteen analyses on 18 zircons from 02QSH06 have U=1556−4866 ppm, Th = 389−852 ppm and Th/U ratio = 0.12−0.38. Fourteen analyses on 15 zircons from 01GD09 have U=475−2148 ppm, Th=315−1256 ppm and Th/U=0.36−0.82 except that HE4.1 analysis shows extremely high Th and U contents (Th = 13044 ppm, U = 6157 ppm). Eighteen analyses on 18 zircons from 02JSH03 give U content of 1257−4552 ppm, Th content of 407−1721 ppm and Th/U ratio of 0.21−0.60.

All analytical zircons for sample 02QSH06 have the ^{206}Pb/^{238}U apparent ages of 222.6−269.0 Ma. However, four analyses of them (HC4.1, HC8.1, HC9.1 and HC17.1) are significantly biased from the normal distribution of the ^{206}Pb/^{238}U apparent ages, and give the abnormal ^{206}Pb/^{238}U apparent ages. Other 14 analyses on 13 grains yield a weighted mean ^{206}Pb/^{238}U age of 245±7 Ma (95% confidence, MSWD=2.83; Fig. 3(a)). For 14 zircons of sample 01GD09, zircon HE4.1 with complex internal structure is probably a relict/inherit grain, and gives the ^{206}Pb/^{238}U apparent age of 293.4±9.0 Ma. Fourteen analyses on other 13 zircons show identical ^{206}Pb/^{238}U ratios within error bar, and give ^{206}Pb/^{238}U apparent ages of 227.1−252.0 Ma. These analyses yield a weighted mean ^{206}Pb/^{238}U age of 241±7 Ma (95% confidence, MSWD=0.93, Fig. 3(b)). ^{207}Pb/^{206}Pb apparent ages for some grains from both samples are inconsistent with the ^{206}Pb/^{238}U and ^{207}Pb/^{235}U apparent ages. The disconcordance is likely related to the higher counting for ^{207}Pb during measurement. Eighteen analyses on 17 zircons for sample 02JH03 have the ^{206}Pb/^{238}U apparent ages of 237.9−261.5 Ma, and yield a weighted mean ^{206}Pb/^{238}U age of 247±6 Ma (95% confidence, MSWD=0.94, Fig. 3(c)). If not considering HA2.1, HA3.1, HA8.1, HA10.1, HA15.1 and HA17.1 analyses with disconcordant ^{206}Pb/^{238}U and ^{207}Pb/^{235}U apparent ages, other twelve analyses yield a weighted mean ^{206}Pb/^{238}U age of 244±6 Ma. On the concordia (Figs. 3(a)−(c)) these analyses on zircons for each sample form a single and tight cluster, indicating that the U-Pb isotopic system of the zircons is closed, and these grains have insignificant Pb-loss and internal redistribution of U after crystallization[17]. Three samples give the weighted mean $^{206}Pb/^{238}U$ ages of 244±4 Ma (n=14, MSWD=1.20, 02QSH06), 239±3 Ma (n=14, MSWD=0.93, 01GD09) and 243±3 Ma (n=18, MSWD=0.94, 02JH03), respectively.

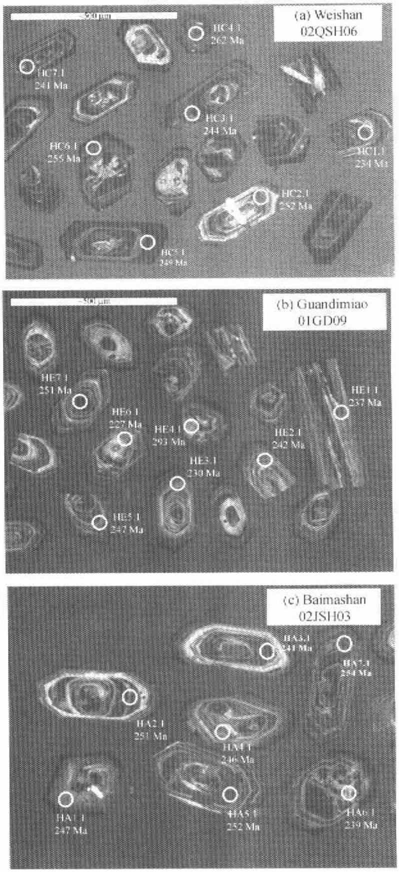

Fig. 2. The cathodoluminescence (CL) image of representative zircons. (a) Tangshi ultraunit for Weishan (01QSH02); (b) Tangshi ultraunit for Guandimiao (01GD09); (c) Longtan ultraunit for Baimashan (02JH03). Circle and number denote the analytical spot, serial number and $^{206}Pb/^{238}U$ apparent age, respectively.

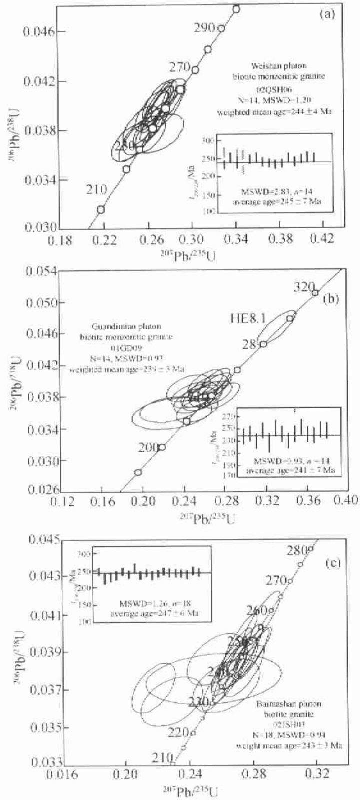

Fig. 3. SHRIMP U-Pb concordia diagram (b) for zircons from the representative granitic samples; (a), (b) and (c) are the same as those in Fig. 2.

4 Discussion

Weishan pluton intruded into Denovian strata and underlay Cretaceous strata. Previously geochronological data for the pluton from mineral K-Ar, whole-rock Rb-Sr, zircon U-Pb and monazite U-Th-Pb methods gave an age range of 193—257 Ma[10—12,15], thus interpreted as Indosinian-early Yanshanian pluton. Previously geochronological data for Tangshi ultraunit of Weishan pluton (mineral K-Ar and zircon U-Pb methods) ranged from 198 Ma to 230 Ma[9—12,15]. Longtan ultraunit of Baimashan pluton intruded Silurian Shuiche untraunit and Neoproterozic-Paleozoic strata, and were dated at 217—267 Ma (mica K-Ar and grain zircon U-Pb). Three typical granites described as above gave the SHRIMP zircon U-Pb ages of 244±4 Ma, 243±3 Ma and 239±3 Ma, respectively, representing the crystallized ages of Tangshi and Longtan ultraunits granites. Xu et al.[13] obtained the single-grained zircon LA-ICPMS U-Pb ages of 239±5 Ma and 236±8 Ma for Luxi and Xiazhuang plutons from Guidong complex at the border of southern Jiangxi and northern Guangdong provinces. The weighted mean $^{206}Pb/^{238}U$ ages of 233, 230 and 236 Ma (SHRIMP zircon U-Pb method) were reported for Darongshan, Jiuzhou and Taima plutons in southeastern Guangxi, which were previously considered to be Hercynian-Indosinian peraluminous granites[14]. Qiongzhong granite in Hainan Province yielded an SHRIMP zircon U-Pb age of 237±3 Ma[1)]. These data indicate that the emplacement of the peraluminous early Indosinian/Hercynian-Indosinian granites as previously thought probably took place in a narrow time interval of 230—244 Ma (early Indosinian episode) and were the derivations of the crustal materials in the same tectonothermal event. Although the Indosinian granites in Nanling Mountains areas exhibit a roughly EW-trending distribution[13], it is most likely that the Indosinian granites within the SCB spatially distribute as planar shape in Hunan, Jiangxi, Guangxi and Guangdong[20] rather than an NE-trending pattern along Hunan and Guangxi as previously thought[9].

The Indosinian tectonic evolution of the SCB and petrogenetic dynamics of these Indosinian granites have long been debated. For example, some researchers considered that the Indosinian tectonic evolution within the SCB was related to early Mesozoic subduction/collision in the areas[3,4], and these Indosinian granites were the derivation from island-arc setting. But this hypothesis has been challenged by the absence of contemporaneous ophiolite suites, oceanic basins and island-arc magmatism within the SCB[21,22]. Other researchers believed that the formation of these Indosinian granites was closely related to the westward subduction of the Pacific plate. But paleomagnetic evidence showed that the westward subduction of the Pacific plate occurred not earlier than 125 Ma[23]. The planar-shaped distribution of the Indosinian granites and the poor development of the contemporaneous volcanic rocks within the SCB also argue against the viewpoints that the petrogenesis of these Indosinian granites was directly associated with the subduction/collision within the SCB and the subduction of the Pacific plate[21]. Recent studies revealed that continental rifting and lithospheric extension were the dominant mechanisms of tectonic evolution of the SCB during Mesozoic[24—27]. However, the Indosinian mafic magmatism (204—224 Ma) is only discovered at Daoxian (gabbroic xenoliths) and Huziyan (alkaline basalts) in southern Hunan Province[28,29]. Additionally, even if there existed the Indosinian magma underplating (revealed by the geochemistry of poorly mafic magmatism during 204—224 Ma) that can induce the formation of the contemporaneous granites[28,30], the thermal equilibrium of the underplating magma with wall rock would take place at the time interval of 5—20 Ma after the magma underplating event[30,31]. That is to say, the generation of the peraluminous granites induced by the magma underplating event should be later than 224 Ma (probably 210—224 Ma). These Indosinian granites in the studied areas, however, were precisely dated at 230—244 Ma, which is earlier than that of the magma underplating event.

It is alterative that formation of these peraluminous granites is the result of crustal thickening induced by tectonic compression during Indosinian episode[14,28]. Present studies show that these granites within the SCB are characterized by strongly to slightly peraluminous (A/CNK>1.00) and potassium-rich (K_2O>3.0%), and have similar Sr-Nd isotopic compositions with the gneisses within the SCB[9—12]. These granites were usually interpreted as the products of the mica-induced dehydrated melting of middle/lower-grade metamorphic rocks in the middle/upper crust[10—12,30]. The numerical modeling results show that the tectonic thickening of the continental crustal materials would result in the significant increasing of the temperature within the crust[30]. The mica-induced dehydration melting of the crustal materials will occur once the thickening factor (crustal thickness after deformation versus initial thickness) is greater than 1.3, producing a large amount of peraluminous granitic melt. Present data show that there developed the shallow marine sediment in Jiangxi, Hunan, Guangxi and Guangdong during late Paleozoic except for the Qin-Fang trough characterized by epicontinental to bathyal clastic sediments. The middle Triassic sequence is commonly absent within the SCB. The lower Triassic sequences downward within the SCB exhibit strongly deformation structures in the areas, e.g. folds and thrust[32,33]. The mica separates for the mylonitic rocks from the thrusting/strike-slip shear zones within the SCB yielded the $^{40}Ar/^{39}Ar$ plateau ages of 249—195 Ma[32—35] (authors' unpublished data). These observations suggest a tectonically crustal thickening event within the SCB during Indosinian episode. The scenario of the tectonically crustal thickening contemporaneous with the generation of the Indosinian granites is also supported by the following observations: (1) the gneissic textures in Tangshi ultraunit for Weishan and

1) See footnote 1) on page 1396.

Guandimiao plutons and Longtan ultraunit for Baimashan pluton; (2) the lentoid quartz dioritic xenoliths hosted in these granitic plutons; (3) the undulatory extinction of quartz and bending of biotite observed in thin sections of these studied samples. These observations suggest that the generation of these plutons was related to the Indosinian compressional regime rather than the extension regime in the area[12,24−27].

Contemporaneous with the formation of the Indosinian granites (230—244 Ma) within the SCB, there are a series of subduction/collision around the SCB. At the northern margin of the SCB, the Yangtze block subducted toward the north during Triassic (~240 Ma) and subsequently collided with the North China Craton along the Dabie-Sulu Orogeny[36−38]. At the southwestern margin of the SCB, the glaucophane separates for glaucophane schist from the Changning-Menglian belt yielded an $^{40}Ar/^{39}Ar$ plateau age of ~270 Ma[39], and the post-collisional igneous rocks from Jinghong, Lincang and Baimaxueshan areas gave the SHRIMP zircon U-Pb ages of 229—241 Ma[40,41] (authors' unpublished data). These geochronological data indicate the subduction of Paleotethys Ocean during Hercynian episode and subsequent collision during Indosinian episode along the Bentong-Raub-Changning-Menglian suture[39,42,43]. At the southern margin of the SCB, the $^{40}Ar/^{39}Ar$ and zircon U-Pb thermochronological data for the metamorphic rocks in central and northern Vietnam (e.g. Song Chay, Day Nui Con Voi, Da Nang-Khe Sanh and Kontum terranes and Truong Son) and northern Thailand imply that the Indochina block clockwisely collided relative to the SCB during Indosinian episode (258—240 Ma in northern Vietnam and ~220 Ma in northern Thailand)[42−45]. These data indicate that the formation of the Indosinian peraluminous granites (230—244 Ma) within the SCB is temporally coupled with the Indosinian Orogen around the SCB. The coupling indicates an intrinsic relationship among them. It is most likely that the convergence of continental margin not only rebuilt/inversed the preexistedly structural pattern within the continent, but also induced the magmatism within the continent[46−50]. The convergence induced geological responses are probably over 1600 km toward the continent as proposed by Ziegler et al.[46]. Consequently, the geochronological data of these Indosinian granites in the studied areas provide important constraints on better understanding the spatiotemporal distribution of the Indosinian granites and early Mesozoic tectonic evolution of the SCB.

Acknowledgements The authors thank two anonymous reviewers and editors for their critical and constructive comments on this paper. We would like to thank Li Xianhua for his helpful discussions. This work was supported by the National Natural Science Foundation of China (Grant Nos. 40334039, 40421303 and 40473019), and the Chinese Academy of Sciences (Grant No. KZCX2-102).

References

1. Deprat, J., Etude des plissements et des zones décrasement de la moyenne et de la basse Rivière Noire, Mèmoire du Service Géologique Indochine, 1914, 3: 59.
2. Fromagat, J., Sur la structure des Indosinides, Comptes Rendus de l'Académie des Sciences, 1932, 195: 538.
3. Hsü, K. J., Li, J. L., Chen, H. H. et al., Tectonics of South China: Key to understanding west Pacific geology, Tectonophysics, 1990, 183: 9—39.
4. Li, J. L., Continental Lithospheric Structure and Geological Evolution in Southeast China (in Chinese), Beijing: Chinese Metallurgic Industry Publishing House, 1993, 47—123.
5. Ren, J. S., Chen, T. Y., Niu, B. G. et al., Continental Lithospheric Evolution and Mineralization in East China and Its Adjacent Areas (in Chinese), Beijing: Science Press, 1990, 1—125.
6. Guo, L. Z., Shi, Y. S., Ma, R. S., On the formation and evolution of the Mesozoic-Cenozoic active continental margin and island arc tectonics of the western Pacific ocean, Acta Geologica Sinica (in Chinese), 1983, 57(1): 51—61.
7. Guo, F. X., Mesozoic-Cenozoic Nanhua (South Chian) orogenic belt: Subaerial tridirectional orogen, Acta Geologica Sinica (in Chinese), 1998, 72(1): 22—33.
8. Deng, J. F., Zhao, H. L., Mo, X. X. et al., Intracontinental subduction of the Yangtze continent and continental reducing: Inferred from muscovite (two mica) granites, Geol. J. Univ. (in Chinese), 1995, 1(1): 50—57.
9. HBGMR, Regional geology survey in Hunan Province (in Chinese), Beijing: Geological Press, 1988, 1—543.
10. Zhuang, J. L., Liu, Z. W., Tan, B. X., Relation of the small rock bodies in southern Hunan to the formation of ore deposits and prognosis of concealed deposits, Hunan Geology (in Chinese), 1988, 4(sup): 1—163.
11. Jia, B. H., Primary studies of emplacement mechanism for Hunan granites, Hunan Geology (in Chinese), 1998, 10(sup): 1—164.
12. Chen, J. F., Jahn, B. M., Crustal evolution of southeastern China: Nd and Sr isotopic evidence, Tectonophysics, 1998, 284: 101—133.
13. Xu, X. S., Deng, P., O'Reilly, S. Y. et al., Single zircon LAM-ICPMS U-Pb dating of Guidong complex (SE China) and its petrogenetic significance, Chinese Science Bulletin, 2003, 48(17): 1892—1899.
14. Deng, X. G., Chen, Z. G., Li, X. H., SHRIMP U-Pb zircon dating of the Darongshan-Shiwandashan, Geological Review (in Chinese), 2004, 50(4): 426—432.
15. Institute of Regional Geological Survey of Hunan, Classification of granitic unit-ultraunit and its mineralization in Hunan Province, Hunan Geology (in Chinese), 1995, 8(supp.): 1—84.
16. Song, B., Zhang, Y. H., Wan, Y. S., Mount making and procedure of the SHRIMP dating, Geological Review (in Chinese with English abstract), 2002, 48(suppl.): 26—30.
17. Williams, I. S., Claesson, S., Isotope evidence for the Precambrian province and Caledonian metamorphism of high grade paragneiss from the Seve Nappes, Scandinavian Caledonides, II, Ion microprobe zircon U-Th-Pb, Contrib. Mineral Petrol., 1987, 97: 205—217.
18. Claoue-Long, J. C., Compston, J., Roberts, C. M. F., Two Carboniferous ages: A comparison of SHRIMP zircon dating with conven-

tional zircon ages and $^{40}Ar/^{39}Ar$ analysis, in Geochronology Time Scales and Global Stratigraphic Correlation 54, SEPM Special Publication, 1995: 3—21.
19. Ludwig, K. R., Sqiud 1.02: A user manual. Berkeley Geochronological Center Special Publiccation, 2001, 1—219.
20. Rowley, D. B., Ziegler, A. M., Nie, G., Comment on "Mesozoic overthrust tectonics in South China". Geology, 1997, 17: 384—386.
21. Gilder, S. A., Gill, J., Coe, R. S. et al., Isotopic and paleomagnetic constraints on the Mesozoic tectonic evolution of South China, J. Geophy. Res., 1996, 107(B7): 16137—16154.
22. Engebretson, D. C., Cox, A., Gordon, R. G., Relative motions between oceanic and continental plates in the Pacific basins, Geol. Soc. Amer. Spec. Paper, 1985, 206: 1—59.
23. Zhou, X. M., My thinking about granite genesis of South China, Geological J. China Univ. (in Chinese), 2003, 9(4): 556—565.
24. Wang, Y. J., Fan, W. M., Peng, T. P. et al., Element and Sr-Nd systematics of early Mesozoic volcanic sequence in southern Jiang Province, South China: Petrogenesis and tectonic implications, International Journal of Earth Sciences, 2005, 43(1): 53—65.
25. Wang, Y. J., Fan, W. M., Guo, F. et al., Geochemistry of Mesozoic mafic rocks around the Chenzhou-Linwu fault in South China: Implication for the lithospheric boundary between the Yangtze and the Cathaysia Blocks, Inter'l Geol. Rev., 2003, 45(3): 263—286.
26. Chen, P. E., Kong, X. G., Wang, Y. X. et al., Rb-Sr isotopic dating and significance of earth Yangshanian bimodal volcanic-intrusive complex from south Jiangxi Province, SE China, Geol. J. China Univ. (in Chinese), 1999, 5(4): 379—383.
27. Li, X. H., Chung, S. L., Zhou, H. W. et al., Jurassic intraplate magmatism in southern Hunan-eastern Guangxi: $^{40}Ar/^{39}Ar$ dating, geochemistry, Sr-Nd isotopes and implications for tectonic evolution of SE China, in Aspects of the Tectonic Evolution of China (eds. Malpas, J., Fletcher, C. J., Aitchison, J. C. et al.), Geol. Soc., Lon., Spec. Pub., 2004, 226: 193—216.
28. Guo, F., Fan, W. M., Lin, G. et al., Sm-Nd dating and petrogenesis of Mesozoic gabbro xenolith in Daoxian County, Hunan Province, Chinese Science Bulletin, 1997, 42: 1814—1817.
29. Zhao, Z. H., Bao, Z. W., Zhang, B. Y., The geochemistry of Mesozoic Basalts in south Hunan Province, South China, Science in China, Ser. D, 1998, 41(sup): 102—112.
30. Wang, Y. J., Zhang, Y. H., Fan, W. M. et al., Numerical modeling for generation of Indosinian peraluminous granitoids Hunan Province: basaltic underplating versus tectonic thickening, Science in China, Ser. D, 2002, 45(11): 1042—1056.
31. Koyaguchi, T., Kaneko, K., A two-stage thermal evolution model of magmas in continental crust, J. Petrol., 1999, 40(2): 241—254.
32. Li, Z. X., Tectonic history of the major East Asian lithospheric blocks since the mid-Proterozoic: A synthesis, in Mantle dynamics and plate interactions in East Asia (eds. Flower, M. F. J., Chung, S. L., Lo, C. H. et al.), Amer. Geophy. Union (Geodynamic series), 1998, 27: 221—243.
33. Chen, A., Mirror-image thrusting in the South China orogenic belt: Tectonic evidence from western Fujian, southeastern China, Tectonophysics, 1999, 305: 497—519.
34. Peng, S. M., Fu, L. F., Zhou, G. Q., Tectonic evolution of Yunkai massif and its shearing anatectic origin of gneissic granitic rocks (in Chinese), Wuhan: China Univ. Geosciences Press, 1995, 1—165.
35. Wang, Y. J., Zhang, Y. H., Fan, W. M. et al., Structual signatures and $^{40}Ar/^{39}Ar$ geochronology of the Indosinian tectonic zone, South China, Jounal of Structual Geology, 2005 (in press).
36. Ames, L., Zhou, G., Xiong, B., Geochronology and isotopic character of ultrahigh-pressure metamorphism with implications for collision of the Sino-Korean and Yangtze cratons, Central China, Tectonics, 1996, 15: 472—489.
37. Li, S. G., Xiao, Y. L., Liou, D. L. et al., Collision of the North China and Yangtze Blocks and formation of coesite-bearing eclogites: Timing and Processes, Chem. Geol., 1993, 109: 89—111.
38. Zhang, K. J., North and South China collision along the eastern and southern North China margins, Tectonophysics, 1997, 270: 145—156.
39. Zhong, D. L., Paleotethyan orogenic belts in Yunnan and western Sichuan (in Chinese), Beijing: Science Press, 1998, 1—230.
40. Jian, P., Liu, D. Y., Sun, X. M., SHRIMP dating of Baimaxueshan and Ludian granitoids batholiths, northwestern Yunnan Province and its geological implication, Acta Geoscientia Sinica (in Chinese), 2003, 24(4): 338—342.
41. Zhao, C. F., Variscan and Indosinian granites in northern Tengchong, Yunnan, Regional Geology of China (in Chinese), 1999, 18(3): 260—263.
42. Metcalfe, I., Gondwanaland orogin, dispersion, and accretion of East and Southeast Asian continental terranes, J. South Amer. Earth Sci., 1994, 7: 333—347.
43. Mo, X. X., Shen, S. Y., Zhu, Q. W. et al., Volcanics-ophiolite and mineralization in the southern Nujiang-Langcangjiang-Jinshajiang area, southwestern China (in Chinese), Beijing: Chinese Geological Publishing House, 1998, 1—128.
44. Carter, A., Roques, D., Bristow, C. et al., Understanding Mesozoic accretion in southeast Asia: significance of Triassic thermotec- tonism (Indosinian orogen) in Vietnam, Geology, 2001, 29(3): 211—214.
45. Lepvrier, C., Maluski, H., van Vuong, N. et al., Indosinian NW-trending shear zone within the Truong Son belt (Vietnam): ^{40}Ar-^{39}Ar Triassic/Cretaceous to Cenozoic overprints, Tectonophyics, 1997, 283: 105—128.
46. Ziegler, P. A., Cloetingh, S., van Wees, J. D., Dynamics of intra-plate compressional deformation: the Alpine forland and other examples, Tectonophysics, 1995, 252: 7—59.
47. Nam, T. N., Toriumi, M., Itaya, T., P-T-t paths and postmetamorphic exhumation of the Day Nui Con Voi shear zone in Vietnam, Tectonophysics, 1998, 290: 299—318.
48. Singharajwarapan, S., Berry, R., Tectonic implications of the Nan suture zone and its relationship to the Sukhothai fold belt, northern Thailand, J. Asian Earth Sci., 2000, 18: 663—673.
49. de Graiansky, P. C., The inverted margin of the French Alps and foreland basin inversion, in Inversion Tectonics (eds. Copper, M. A., Williams, M.), London: Geol. Assoc. Lond. Spec. Pub., 1989, 44: 41—59.
50. Kieinschrodt, K., Voll, G., Deformation and metamorphic evolution of a large-scale fold in the lower crust: the Dembara synforms, Sri Lanka, J. Struc. Geol., 1994, 16(11): 1495—1508.

(Received January 7, 2005; accepted March 29, 2005)